RJC

RASĀYAN *J. Chem.*
Vol. 17 | No. 3 |767-775| July - September | 2024
ISSN: 0974-1496 | e-ISSN: 0976-0083 | CODEN: RJCABP
http://www.rasayanjournal.com
http://www.rasayanjournal.co.in

MILD-CARBON STEELS AS A STORAGE TANK MATERIAL FOR BIODIESEL PRODUCT: A CORROSION ASSESSMENT

V. A. Fardilah[1], Y. M. Pusparizkita[2], M. Tauviqirrahman[1], J. Jamari[1] and A. P. Bayuseno[1,] ✉

[1]Department of Mechanical Engineering, Diponegoro University, Semarang, 50275, Indonesia
[2]Department of Environmental Engineering, Diponegoro University, Semarang 50275, Indonesia
✉Corresponding Author: apbayuseno@gmail.com

In the practice of biodiesel storage tanks, there are questions about their long-term viability for handling and storage. This study examined the effects of biodiesel blends containing B0, B30, B40, and B100 products on the corrosion resistance of carbon steels graded AISI 1020 and AISI 1045. Static corrosion tests for 168 hours at 25°C were performed by immersing test coupons of each carbon steel in the biodiesel blending solution. An electrochemical analysis revealed that the AISI 1020 and AISI 1045 coupons had current density (*Icorr*) values higher than 0.1 μA/cm^2. In various biodiesel blends, the corrosion rates for AISI 1020 and AISI 1045 increased from 0.02275 to 0.051184 *mmpy* and from 0.04777 to 0.05890 *mmpy*, respectively. The results show that mild steels used to store biodiesel have a limited ability to resist corrosion. The oxygen content of biodiesel may affect the corrosion products of mineral rusts (Fe_2O_3, Fe_3O_4) on steel surfaces. Because of its significantly higher oxygen content, steel-AISI 1045 has a faster corrosion rate than steel-AISI 1020. The study findings could provide a technical explanation for the corrosive nature of biodiesel storage tanks.

Keywords: Corrosion rate; Mild-carbon steel; Biodiesel blends; Electrochemical analysis; Mineral Rusts.
RASĀYAN *J. Chem.*, Vol. 17, No.3, 2024

INTRODUCTION

Most biodiesel produced in Indonesia today is made from palm oil and blended with Petro diesel; the mixture has been referred to as Bxx, with xx representing the volume percentage of biodiesel.[1] B30, for example, is a blend of 30% biodiesel and 70 % petrol diesel. B100-biodiesel products are for completely replacing Petro diesel. Biodiesel is now more widely used in Indonesia, ranging from B2 to B30 (by decree ESDM No. 12 of 2015). Practically, biodiesel is a good fuel for any diesel engine that requires only minor modifications. Many diesel engines constructed before the early 1990s include natural rubber seals and other components that disintegrate when exposed to biodiesel.[1] Biodiesel has less energy per gallon (124000 BTU) than petrol diesel (136000 BTU/gallon). However, biodiesel with a higher cetane number than Petro diesel exhibits improved ignition properties.[2] In particular, biodiesel is both environmentally friendly and non-toxic.[3-5] Further, biodiesel's oxygen content can cause it to oxidize and contaminate itself during distribution and storage[6–9], as well as corrode metallic parts like the fuel tank and piston heads.[10] Storage tanks are typically made of mild-carbon steel due to their high durability, tensile strength, and low cost.[11] The main disadvantage of mild-carbon steel is its low corrosion resistance. Approximately 80% of biodiesel storage tank systems may be prone to moderate-to-severe corrosion.[12] In most cases, it is more cost-effective to use mild-carbon steel for the storage tank with adequate corrosion protection.[8] Knowing the steel corrosion mechanism in contact with biodiesel is essential for designing, coating, adding inhibitors, cathodic protection, passivating, and choosing materials for steel storage tanks that will withstand corrosion attacks, extending the storage tank lifetime. Despite the complex mechanisms underlying corrosive biodiesel environments in storage tanks, a laboratory study can investigate corrosion in biodiesel settings. This laboratory experiment features a short testing period, low experimental cost, ease of operation, and high reproducibility.[13] Correspondingly, this study proposed that mild-carbon steel corrosion was linked to moisture absorption, microbial oxidation, other pollutants, and condensed water from biodiesel during storage, transportation, and use. Peroxides, hydroperoxides, and monocarboxylic acids are byproducts of biodiesel oxidation that raise the total acid number and lead to mild-carbon steel tanks corroding more quickly.

http://doi.org/10.31788/RJC.2024.1738804

The current study presents a biodiesel corrosion experiment using AISI 1020 and AISI 1045 carbon steels in simulated biodiesel. This research employed electrochemical measurements, gravimetric analysis, scanning electron microscopy (SEM/EDX), and X-ray diffraction (XRD). The results can help choose the right material and prevent corrosion in tanks used to store biodiesel.

EXPERIMENTAL

Biodiesel Corrosion Medium and Test Coupons

Blended using different proportions (v/v) of biodiesel B100 FAME (fatty acid methyl ether) provided by APROBI (Indonesia Biofuel Producer Association) through PT Wilmar, is petroleum-based oil (Pertamina-DEX). Previous studies have investigated the properties of biodiesel and commercial petrodiesel.[14] This biodiesel blend represents B0, B30, B40, and B100 for corrosion testing. Table-1 presents the chemical compositions of AISI 1020 and AISI 1045 steels as electrodes. Before each experiment, the coupons were abraded with 1200-grade SiC paper, defatted with acetone, rinsed with distilled water, and dried before immersion.

Table-1: AISI 1020 and 1045 Carbon Steel Coupons

Steel (wt.%)	C	Mn	P	S	Si	Cr	Ni	Cu	Mo	Fe
AISI 1020	0.2	1.067	0.025	0.024	0.24	-	-	-	-	Balance
AISI 1045	0.45	0.65	0.010	0.008	0.22	0.12	0.01	0.02	-	Balance

Electrochemical Measurements

The Tafel technique, using a potentiostat or galvanostat (CorrTest-Type CS300), assessed the corrosion behavior and rate of two AISI 1020 and AISI 1045 carbon steel sheets after 168 hours of immersion in biodiesel. This NaCl electrolyte promotes an oxidation-reduction reaction while completing the electrical circuit between the anode and cathode. Because biodiesel is not an electrolyte, a solution for electrochemical measurements did not contain biodiesel. Alternatively, the electrochemical experiments used three-electrode cells in a solution with a 3.5% NaCl concentration. The cell was composed of three sections: a carbon steel coupon served as the working electrode (WE); instead, platinum and silver-silver chloride (SSCE) and Ag/AgCl electrodes were used as the counter (CE) and reference (RE) electrodes, respectively. As samples of B0_1020, B30_1020, B40_1020, and B100_1020; and B0_1045, B30_1045, B40_1045, and B100_1045, respectively, are the rusted carbon steel coupons (AISI 1020 and 1045) in concentrations of biodiesel (B0, B30, B40, and B100). Corrosion potential (*Ecorr*), corrosion current density (*Icorr*), and Tafel slopes (anodic-βa and cathodic-βc) are the corrosion parameters observed during the study. The electrodes were all arranged in perfect triangle geometry and faced each other. Figure 1 shows the electrochemical cell test setup.

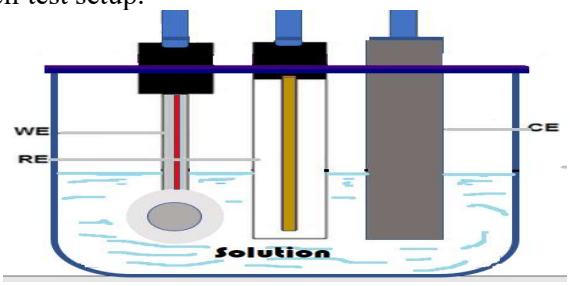

Fig.-1: Potentiostat Setup for Corrosion Test

Faraday's law states that the corrosion rate of an anode is proportional to its corrosion current. The area weight loss typically represents the corrosion and depletion rate, with *mmpy* (millimeter per year) being the most commonly used unit. Equation 1 describes the relationship between current density and corrosion rate:[15]

$$R = 0.129 \frac{i_{corr}\,(E_w)}{\rho}\, mmpy$$

Where the R = corrosion rate (*mmpy*), *Icorr* = corrosion current density (μA/cm^2), Ew = equivalent weight (grams/equivalent) and ρ = density (g/cm^3).

Characterization of Corroded Carbon Steel

A scanning electron microscope with energy dispersive spectroscopy (SEM/EDX) (FEI Quanta 650 FEG) captured high-resolution images of the rusted coupons after 168 hours of immersion. Semi-quantitative X-ray microanalysis was performed at nanometer resolution (with a magnification range of 5–1,000,000x) using conductive and non-conductive specimens. On the corroded samples, X-ray diffraction (XRD) was carried out using Cu-Kα radiation (λ = 0.154 nm) at an angle 2θ range of 10-90°. Furthermore, the QualX-search-match software used the XRD line-matching method for phase identification analysis.[16] The XRD Rietveld method confirmed the finding of rusting minerals using the program Fullprof-2k (version 3.30).[17] The crystal structure model from the COD (Crystallography Open Database) had to be adjusted to fit the profiles.[18]

RESULTS AND DISCUSSION

Tafel Polarization Measurement

Tafel polarization measurements were subjected to AISI 1020 and 1045 cathodic and anodic processes in a 3.5% NaCl solution to assess the effect of biodiesel blend concentration on corrosive steels. The Tafel plots in Fig.-2 demonstrated significant alterations following 128 hours of contact with test coupons containing different biodiesel products. These included changes in the location of Ecorr and the magnitudes of the anodic and cathodic overpotentials. Specimens B0_1020, B30_1020, B40_1020, and B100_1020 all show a discernible leftward (anodic) displacement in Ecorr (Figure 2a), with B40_1020 showing a high mark shift to the left. On the other hand, Ecorr significantly shifted to the left (cathodic) upon applying test coupons B100_1045 (Fig.-2b). Figure-2's Tafel plots illustrate the displacement in Ecorr, while the resting potential vs. time plots show the steady-state potential shifting. Both plots point in the same direction. Biodiesel blended at a higher percentage led to higher corrosion rates of B100_1045. A shift to the right in the color value indicates a more corrosive contribution.[19]

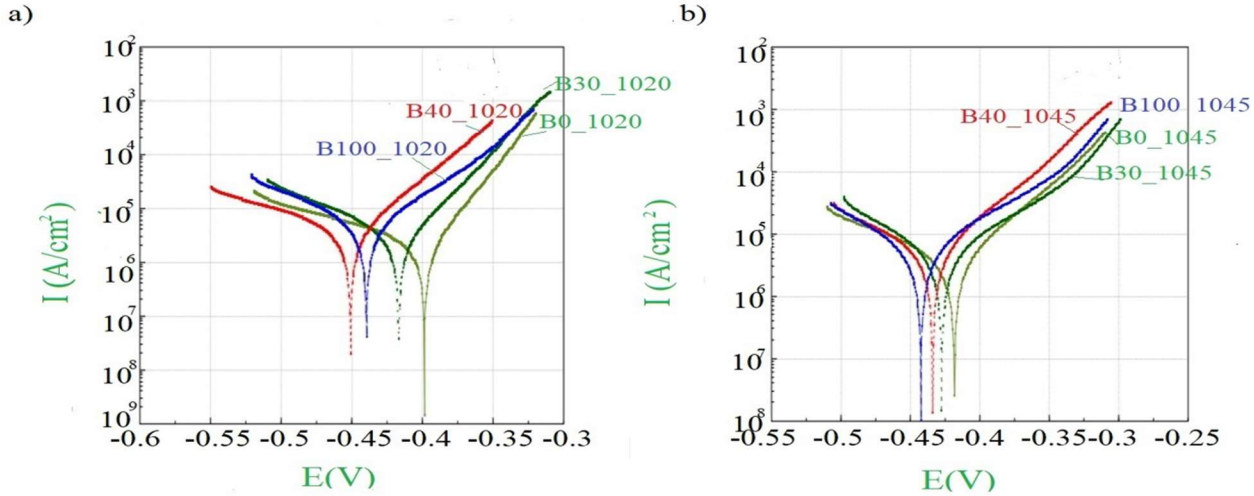

Fig.-2: Cathodic and Anodic Polarization (Tafel) Plots Recorded for a) AISI 1020 Specimens (B0_1020, B30_1020, B40_1020 and B100_1020); b) AISI 1045 Specimens (B0_1045, B30_1045, B40_1045 and B100_1045) in 3.5% NaCl Concentration

Using the linear components of the anodic and cathodic reactions, *Icorr* was calculated.[20] Table-2 summarizes the electrochemical kinetic parameters derived as a function of alloy composition from such mathematical treatments and the corrosion rates computed using the Tafel extrapolation method. In regions of current density [*Icorr* > 1 (μA/cm^2)] and corrosion rate (R > 0.01 *mmpy*) related to corrosion level, all specimens showed high corrosion.[21] As a result, the biodiesel product interacting with B0_1020, B30_1020, B40_1020, and B100_1020 surface AISI 1020 steel provided *Icorr* values ranging from 1.959 to 4.4065 μA/cm^2, indicating a high degree of corrosion. Instead, the behavior of B0_1045, B30_1045, B40_1045, and B100_1045 specimens maintain similar behavior for the interaction with biodiesel products, having *Icorr* values in the zone of high corrosion level and showing current density in ranges of 4.1131 to 5.0709 μA/cm^2.

Table-2: Corrosion Analysis Results of AISI 1020 and AISI 1045 Steel in B0, B30, B40, and B100 Products

No.	Test specimen	Corrossion rate (*R*) (*mmpy*)	Current density (*Icorr*)(μA/cm^2)	Potential (mV)	βa (mV)	βc (mV)	Residual
1	B0_1020	0.022769	1.959	-398.23	33.868	125.34	1.2808
2	B30_1020	0.027881	2.3988	-416.41	39.439	80.601	9.0425
3	B40_1020	0.045886	3.9478	-450.69	51.758	131.04	3.4952
4	B100_1020	0.051364	4.4065	-439.28	59.874	86.39	6.4899
5	B0_1045	0.047944	4.1131	-418.03	57.708	121.05	8.66
6	B30_1045	0.049489	4.2456	-427.16	70.357	76.814	1.458
7	B40_1045	0.055891	4.7949	-433.69	54.772	91.703	7.518
8	B100_1045	0.059109	5.0709	-442.17	74.326	80.997	1.181

Moreover, the B100_1020 specimen, which has the highest corrosion rate value of 0.051364 *mmpy* compared to the B0_1020 specimen, which has the lowest corrosion rate value of 0.022835 *mmpy*, shows that a higher percentage of biodiesel with FAME vegetable oil increases the corrosion rate of AISI 1020 steel. Figure-2 illustrates that the Fe-anodic dissolution in 3.5% NaCl follows Tafel's rule as FAME levels rise. Short-term laboratory tests in a simulated environment are possibly unreliable for forecasting long-lasting corrosion rates.[22] In AISI 1045 carbon steel, the corrosion rate increased similarly to that of biodiesel. The corrosion rate values obtained from B0_1045, B30_1045, B40_1045, and B100_1045 are 0.047944, 0.049489, 0.055891, and 0.059109 *mmpy*, respectively. Despite increasing biodiesel percentages, AISI 1020 carbon steel had higher corrosion performance than AISI 1045, indicating a low level of corrosion. Given chlorite corrosion, AISI 1020 steel has a low corrosion rate, while AISI 1045 steel has a high corrosion rate. However, AISI 1020 and AISI 1045 storage materials have low resistance to biodiesel corrosion, with values greater than 0.1 (μA/cm^2), making it challenging for biofuel storage. Using galvanized or coated steels may improve the sustainability of biodiesel storage tanks.[23]

Characterization of Corrosion Products from AISI 1020 and AISI 1045 Following Exposure to B40 and B100 Blends

In this study, the characterization of corrosion products was focused on B40_1020, B40_1020, B40_1045, and B100_1045 because they had higher corrosion rates than the other specimens studied. Figure-3a depicts the surface morphology of B40_1020 and B40_1020 after 168 hours of exposure to B40 and B100 products, where iron oxides caused localized corrosion. Furthermore, the steel surface has "craters," indicating that corrosion product formation began in areas with localized corrosion, relating to the accumulated pressure of the gases within the metallic surface until they burst, allowing oxygen to enter and form oxide.[24] The EDX analysis also revealed the chemical elements contained in the corroded specimens, as shown in Fig.-3a and 3b. Surface elements such as O, C, and Fe indicated the presence of fatty acid salts, carbonates, hydroxides, oxyhydroxides, and iron oxides.[25] Rather, the presence of elements like Ca, Cl, Si, and S connects the chemical compositions of the carbon steel specimens. The pitting corrosion caused by corrosion attack exhibits a notable concentration of different oxides, suggesting that the B40_1020 (26.0%) and B100_1020 (23.1%) specimens have a high oxygen content. Because of its hygroscopicity, biodiesel can absorb water and CO_2 from the atmosphere, potentially producing oxygen-forming oxides.[26] The presence of water in the biodiesel is also due to hydrolysis and oxidation events occurring during the testing period. Increasing immersion time promotes increased oxygen concentration because of the various types of fatty and organic acids formed during biodiesel oxidation processes, which can accelerate corrosion.[27]
The oxidation of biodiesel resulted in the production of RCOO-radicals, which in turn caused the carbon content of the corrosion products B40_1020 and B100_1020 to increase from 8.0 % to 21.1 %, respectively.[25] Additionally, carbon is present in corrosion products, which are the byproduct of the breakdown of fatty acids and other acidic substances that react with metallic oxides to form organic deposits.[28] Following 185 hours of immersion in the test biofuels, Fig.-4a and b depict the localized corrosion of B40_1045 and B100_1045. This material has images showing isolated, dispersed patches of corrosion.[29] Different corrosion products with higher mass losses than those in B40_1045 relate to the deteriorating corrosion condition. As indicated by the presence of O, C, and Fe in the EDX spectra of both specimens, the metal surface may contain fatty acid salts, iron oxides, hydroxides, oxyhydroxides, and

carbonates. When biodiesel oxidized and produced RCOO-radicals, the carbon content of corrosion products B40_1045 and B100_1045 dropped from 24.9% to 16.8% due to the environmental absorption of CO2.25 These results also demonstrate that the B100_1045 specimens, which had a higher carbon content (0.45 wt.%) than the B100_1020 specimen, showed significant corrosion behavior responses to biodiesel.

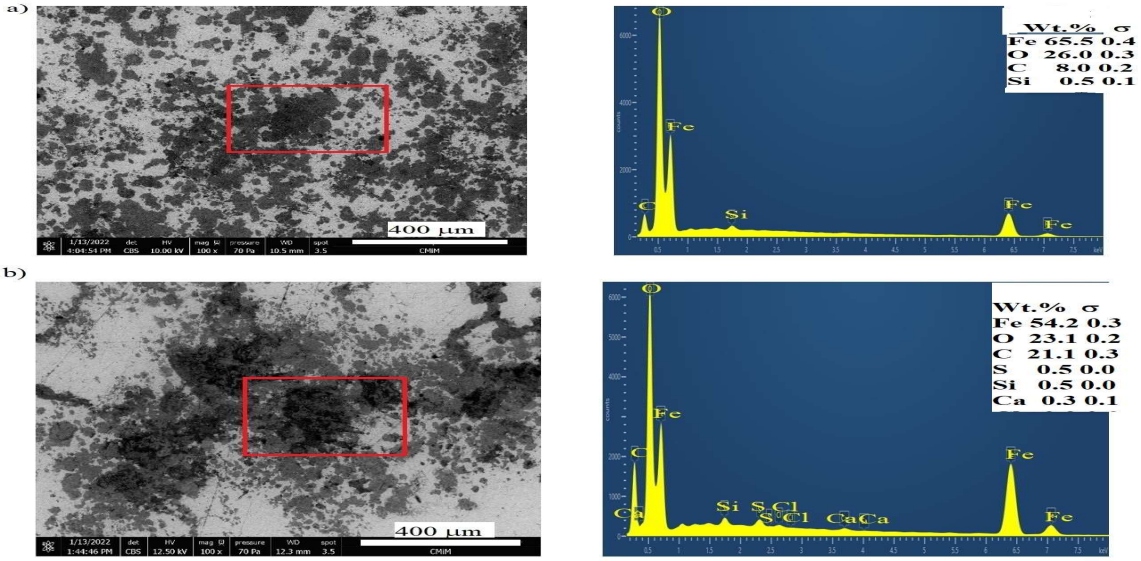

Fig.-3: Surface Morphologies and Chemical Compositions (SEM/EDS analysis) of Corroded Surfaces of a) B40_1020, b) B100_1020 Specimens after 168 hours Immersion in Biodiesel Product

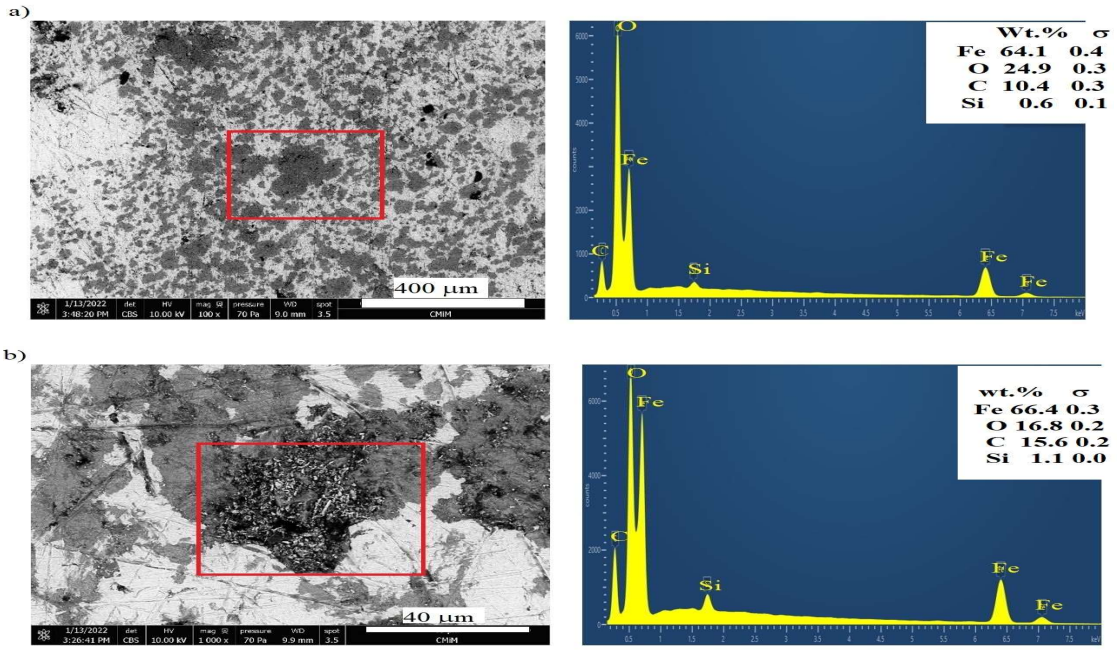

Fig.-4: Surface Morphologies and Chemical Compositions (SEM/EDX analysis) of Corroded Surfaces of a) B40_1045; b) B100_1045 Specimens after 168 hours Immersion in Biodiesel Product

The XRD Rietveld characteristic plot of test coupons exposed to the B40 product for 168 hours is in Fig.-5. The low spectra suggest a thin layer of rust. The presence of siderite (COD#1548824: $FeCO_3$), hematite (COD#2108027: α-Fe_2O_3), magnetite (COD#1539747: Fe_3O_4), and lepidocrocite (COD#2108027: γ-FeOOH) was confirmed as revealed by XRD analysis of the corrosion products for specimens a) B40_1020 and b) B40_1045.[30] These hydroxides and oxides are created when iron reacts with oxygen or water. Here, oxygen can act as an electron acceptor for corrosion products like iron oxides (Fe_2O_3 and Fe_3O_4).[31]

Moreover, $FeCO_3$ may result from the interactions between iron, RCOO, and COOH radicals generated by methyl esters and fatty acids in biodiesel radicals. B40_1045 carbon steel submerged in B40 showed a 17.9 % increase in corrosion rate after 168 hours, indicating the formation of a protective oxide layer on the metal's surface that included magnetite and siderite. Magnetite with small crystal sizes tends to concentrate in the core layers of rust due to a lack of oxygen. After 168 hours of immersion in biodiesel, carbon steel corrosion products can follow the process.[25,32]

$$4Fe + 3O_2 \rightarrow 2Fe_2O_3 \quad (1)$$

$$4Fe + 2O_2 \rightarrow 4H_2O \quad (2)$$

$$4Fe(OH)_2 + O_2 \rightarrow 2Fe_2O_3 \cdot H_2O + 2H_2O \quad (3)$$

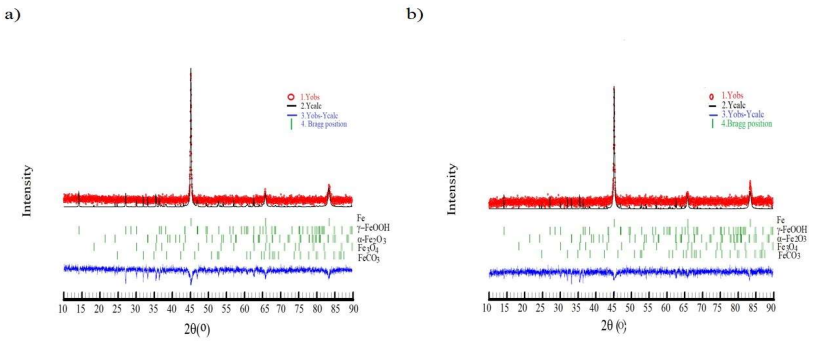

Fig.-5: XRD Rietveld Plots of Corroded Surfaces for Specimens a) B40_1020 and b) B40_1045

Significant Finding of the Present Study

Metallic corrosion is related to both its anodic behavior and the corrosive electrolyte. Measuring the electrochemical corrosion of metals in biodiesel is impossible because it is not an electrolyte.[33] As a result, there are limited investigations into the electrochemical corrosion of metals in biodiesel.[19,34] In this testing, biodiesel-corroded carbon steel contained 3.5% sodium chloride. The generated rusting mineral included $Fe(OH)_2$ at the electrode surface, while the inner layer had Fe_2O_3 and Fe_3O_4. The concentration of contaminants in biodiesel considerably influenced its electrochemical corrosivity. Corrosion current density and corrosion potential fluctuate with biodiesel purity.[35] The electrolyte's ohmic potential dips appeared to have a significant impact on the observed polarization curves and impedance data.[35] The formation of adherent corrosion compounds on a metal surface may reduce the electrochemical activity on the metal surface.[36] The results also demonstrated that both the temperature and the level of biodiesel blends affected the moisture absorption of biodiesel and Petro-diesel blends. The hygroscopicity of biodiesel is higher than that of diesel.[12] Furthermore, the corrosion rate observed without biodiesel is lower than that observed with biodiesel blends of B30, B40, and B100. The corrosion rate increased in concentration as the amount of biodiesel increased. When exposed to biodiesel, the oxygen concentration is higher than when exposed to petrol diesel, making biodiesel more corrosive due to fatty acids. The corrosion data also confirmed that AISI 1020 and AISI 1045 carbon steels had higher corrosion rates at B100 (100% biodiesel) of 0.051364 and 0.059109 *mmpy*, respectively. Similarly, carbon steel is prone to corrosion in industrial applications such as fuel handling and storage. Approximately 80% of biodiesel storage tanks can fail due to corrosion at a minimum-to-high rate; the present finding suggests that corrosion of AISI 1020 and AISI 1045 might suffer at a severe (high) rate when used for storage materials.[37] A protective coating on carbon steel may improve its corrosion resistance. For instance, higher chromium (Cr) and molybdenum (Mo) content may improve corrosion resistance.[38] However, corrosion can still occur at varying profiles and rates.[39,40] This behavior may relate to a change in the physical properties of the stored fuel, particularly with higher-concentration biodiesel blends.[41] This interaction complexity must be better defined and explained. The corrosion of carbon steel against biodiesel on various steel protective layers requires more research.

CONCLUSION

In this work, the uniform corrosion type mainly occurred in all carbon steel specimens. The corrosion rate decreased in B30, B40, and B100 products, resulting in a higher concentration of biodiesel. The oxygen

concentration in diesel fuel makes biodiesel more corrosive due to fatty acids. The EDX analysis also showed that the oxygen content in the B100_1020 and B100_1045 products is approximately 24.9 wt.% and 26 wt.%, respectively, whereas the sample in the B40_1020 and B40_1045 products is about 16.8 wt.% and 23.1 wt.%. This biodiesel corrosion might be related to chemical corrosion products such as salts and metal oxides (Fe_2O_3 and Fe_3O_4). The following degradation sequence was consistent across all 168-hour tests. B0-100% diesel is less prone to corrosion. B100 > B40 > B30 > B0 is the order of degradation. Future research must consider the type of corrosion and the need for storage tanks to determine the corrosion rate of each coating specimen.

ACKNOWLEDGMENTS

The authors would like to thank Diponegoro University for the financial support provided through the high-reputation publication of an international journal (RBIT) in the years 2022-2024 under grant contract 225-48/UN7D2/PP/IV/2023.

CONFLICT OF INTERESTS

The authors declare that there is no conflict of interest.

AUTHOR CONTRIBUTIONS

All the authors contributed significantly to this manuscript, participated in reviewing/editing, and approved the final draft for publication. The research profile of the authors can be verified from their ORCID IDs, given below:

Vivi A. Fardilah https://orcid.org/0009-0006-1126-3940
Yustina Metanoia Pusparizkita https://orcid.org/0000-0003-3410-0600
Mohammad Tauviqirrahman https://orcid.org/0000-0003-2694-4184
J. Jamari https://orcid.org/0000-0002-6172-2635
Athanasius P. Bayuseno https://orcid.org/0000-0002-0882-4480

REFERENCES

1. A. Alcántara-Carmona, F.J. López-Giménez, and M.P. Dorado, *Fuel,* **307**, 121788(2022), https://doi.org/10.1016/j.fuel.2021.121788
2. A. P. Bora, D. P. Gupta, and K. S. Durbha, *Fuel,* **259**, 116262(2020), https://doi.org/10.1016/j.fuel.2019.116262
3. D.H. Qi, and C.F. Lee, *Journal of the Taiwan Institute of Chemical Engineers,* **45(2),** 504(2014), https://doi.org/10.1016/j.jtice.2013.06.021
4. G. Knothe, and L.F. Razon, *Progress in Energy and Combustion Science,* **58**, 36(2017), https://doi.org/10.1016/j.pecs.2016.08.001
5. D. Chandran, *In Renewable Energy,* **147(P1)**, 89(2020), Elsevier Ltd, https://doi.org/10.1016/j.renene.2019.08.040
6. F. Sundus, M.A. Fazal, and H.H. Masjuki, *Renewable and Sustainable Energy Reviews,* **70**, 399(2017), https://doi.org/10.1016/j.rser.2016.11.217
7. M.A. Fazal, N.R. Suhaila, A.S.M.A. Haseeb, and S. Rubaiee, *Journal of Cleaner Production,* **181,** 508(2018), https://doi.org/10.1016/j.jclepro.2018.01.248
8. X.P. Nguyen, and H.N. Vu, *International Journal of Renewable Energy Development,* **8(2)**, 119 (2019), https://doi.org/10.14710/ijred.2023.54612
9. F. Cardeño, M. Lapuerta, L. Rios, and J.R. Agudelo, *Renewable Energy,* **159**,1243(2020), https://doi.org/10.1016/j.renene.2020.06.079
10. A.S.M.A. Haseeb, H.H. Masjuki, L.J. Ann, and M.A. Fazal, *Fuel Processing Technology,* **91(3)**, 329(2010), https://doi.org/10.1016/j.fuproc.2009.11.004
11. Y.M. Pusparizkita, T. Setiadi, and A. Harimawan, *MATEC Web of Conferences*, **156**, 01008(2018), https://doi.org/10.1051/matecconf/201815601008

12. M. A. Deyab, and S. T. Keera, *Journal of the Taiwan Institute of Chemical Engineers,* **68**, 187(2016), https://doi.org/10.1016/j.jtice.2016.08.035
13. L. M. Baena, and J. A. Calderon, *Heliyon* **6,** e03735(2020), https://doi.org/10.1016/j.heliyon.2020.e03735
14. V.A. Fardilah, Y. M. Pusparizkita, M. Tauviqirrahman and A.P. Bayuseno, *IOP Conference Series Earth and Environmental Science,* **1268**, 012057(2023), https://doi.org/10.1088/1755-1315/1268/1/012057
15. M.G. Fontana, Corrosion Engineering, McGraw-Hill Co., 3rd Edition, 1987.
16. A. Altomare, C. Cuocci, C. Giacovazzo, A. Moliternia, and R. Rizzia, *Journal of Applied Crystallography,* **41**, 815(2008), https://doi.org/10.1107/S0021889808016956
17. J. Rodriguez-Carvajal, Program Fullprof.2k, version 3.30, Laboratoire Leon Brillouin, France, June 2005.
18. S. Grazulis, D. Chateigner, R.T. Downs, A.F.T. Yokochi, M. Quiros, L. Lutterotti, E. Manakova, J. Butkus, P. Moeck, and A. Le Bail, *Journal of Applied Crystallography,* **42**, 1(2009), https://doi.org/10.1107/S0021889809016690
19. S. Deshpande, A. Joshi, S. Vagge, and N. Anekar, *Materials Today: Proceedings,* **28(2),** 684(2020), https://doi.org/10.1016/j.matpr.2019.12.277
20. Y. Yi, P. Cho, A. Al Zaabi, Y.Addad, and C. Jang, *Corrosion Science,* **74**, 92(2013), https://doi.org/10.1016/j.corsci.2013.04.028
21. H.A. Ariza-Figueroa, J. Bosch, M.A. Baltazar-Zamora, R. Croche, G.S. Hurtado, L. Landa-Ruiz, J.M. Mendoza-Rangel, J.M. Bastidas, F. Facundo Almeraya-Calderón, and D.M. Bastidas, *Materials,* **13**, 2412(2020), https://doi.org/10.3390/ma13102412
22. E. McCafferty, *Corrosion Science,* **47(12),** 3202(2005), https://doi.org/10.1016/ j.corsci.2005.05.046
23. C.L. Kugelmeier, M.R. Monteiro, R. da Silva, S.E. Kuri, V.L. Sordi, and C.A. Della Rovere, *Energy* **226**, 120344(2021), https://doi.org/10.1016/j.energy.2021.120344
24. S. Klimas, K. Fruzzetti, C. Turner, P. Balakrishnan, G. Strati, and R. Tapping, *Heat Exchanger Fouling and Cleaning: Fundamentals and Applications,* pp.302(2003), Available: http://dc.engconfintl.org/heatexchanger/37.
25. E. Hu, Y. Xu, X. Hu, L. Pan, and S. Jiang, *Renewable Energy,* **37(1),** 371(2012), https://doi.org/10.1016/j.renene.2011.07.010
26. M. Fazal, A. Haseeb, and H. Masjuki, *Corrosion Science,* **67**, 50(2013), https://doi.org/10.1016/j.corsci.2012.10.006
27. R. N. de Andrade Ávila, and J. R. Sodré, *Industrial Crops and Products,* **38**, 54(2012), https://doi.org/10.1016/j.indcrop.2012.01.007
28. L.P. Aquino, R.P.B. Hernandez, D.L. Chicoma, H.P.F. Pinto, and I.V. Aoki, *Fuel,* **102,** 795(2012), https://doi.org/:10.1016/j.fuel.2012.06.011
29. D. Jin, X. Zhou, P. Wu P, J. Li, and Ge Hongliang, *Renewable Energy,* **81**, 457(2015), https://doi.org/10.1016/j.renene.2015.03.022
30. E.C. Zuleta, L. Baena, L.A. Rios, and J.A. Calderón, *Journal of the Brazilian Chemical Society,* **23(12)**, 2159(2012), https://doi.org/10.1590/S0103-50532012001200004
31. Y.M. Pusparizkita, W.W. Schmahl, T. Setiadi, B. Ilsemann, M. Reich, H. Devianto, and A. Harimawan, *Journal of Engineering and Technological Sciences,* **52(3)**, 370(2020), https://doi.org/10.5614/j.eng.technol.sci.2020.52.3.5
32. M. A. Fazal, A. S. M. A. Haseeb, and H. H. Masjuki, *Energy,* **40(1),**76(2012), https://doi.org/10.1016/j.energy.2012.02.026
33. J. S. Lee, R. I. Ray, and B. J. Little, *Biofouling,* **26(6)**,623(2010), https://doi.org/10.1080/08927014.2010.504984
34. W. Wang, P.E. Jenkins, and Z. Ren, *Corrosion Science,* **57** 215(2012), https://doi.org/10.1016/j.corsci.2011.12.015
35. L. Díaz-Ballote, J.F. López-Sansores, L. Maldonado-López, and L.F. Garfias-Mesias, *Electrochemistry communications,* **11(1)**,41(2009), https://doi.org/10.1016/j.elecom.2008.10.027
36. M.A. Fazal, S. Rubaiee, and A. Al-Zahrani, *Fuel Processing Technology* **196**, 106178(2019),

https://doi.org/10.1016/j.fuproc.2019.106178
37. P. Bennett, *Materials Today,* **30,** 103(2019), https://doi.org/10.1016/j.mattod.2019.09.019
38. S.M. Hussaini, S.K. Singh, and A.K. Gupta, *Journal of King Saud University, Engineering Sciences*, **26(2)**, 184(2014), https://doi.org/10.1016/j.jksues.2013.05.001
39. L.N. Komariah, S. Arita, B.E. Prianda, and T.K. Dewi, *Journal of King Saud University, Engineering Sciences,* **35(3)**, 232(2023), https://doi.org/10.1016/ j.jksues.2021.03.016
40. H. Tang, N. Abunasser, A. Wang, B.R. Clark, K. Wadumesthrige, S. Zeng, M. Kim, S.O. Salley, G. Hirschlieb, J. Wilson, and K.Y. Simon Ng, *Fuel,* **87(13–14)**, 2951(2008), https://doi.org/10.1016/j.fuel.2008.04.029
41. E. Torsner, *Corrosion Engineering, Science and Technology,* **45,** 42(2010), https://doi.org/10.1179/147842209X12579401586726

[RJC- 8804/2024]